Received: 2 May 2019 | Revised: 25 July 2019 | Accepted: 28 July 2019

DOI: 10.1111/jbi.13689

RESEARCH PAPER

Journal of Biogeography | WILEY

A topoclimate model for Quaternary insular speciation

Víctor García-Olivares[1,2] | Jairo Patiño[1,3] | Isaac Overcast[4,5] | Antonia Salces-Castellano[1,2] | Unai López de Heredia[6] | Fernando Mora-Márquez[6] | Antonio Machado[7] | Michael J. Hickerson[4,5,8] | Brent C. Emerson[1]

[1]Island Ecology and Evolution Research Group, Institute of Natural Products and Agrobiology (IPNA-CSIC), La Laguna, Tenerife, Canary Islands, Spain

[2]School of Doctoral and Postgraduate Studies, University of La Laguna, La Laguna, Tenerife, Canary Islands, Spain

[3]Plant Conservation and Biogeography, Departamento de Botánica, Ecología y Fisiología Vegetal, Universidad de La Laguna, La Laguna, Spain

[4]Biology Department, City College of New York, New York, NY, USA

[5]The Graduate Center, City University of New York, New York, NY, USA

[6]GI Sistemas Naturales e Historia Forestal, Dpto. Sistemas y Recursos Naturales, ETSI Montes, Forestal y del Medio Natural, Universidad Politécnica de Madrid, Madrid, Spain

[7]c/Chopin 1, Tenerife, Canary Islands, Spain

[8]Division of Invertebrate Zoology, American Museum of Natural History, New York, NY, USA

Correspondence
Brent C. Emerson, Island Ecology and Evolution Research Group, Institute of Natural Products and Agrobiology (IPNA-CSIC), C/ Astrofísico Francisco Sánchez 3, La Laguna, Tenerife, Canary Islands 38206, Spain.
Email: bemerson@ipna.csic.es

Funding information
Ministerio de Economía y Competitividad, Grant/Award Number: CGL2013-42589-P, CGL2017-85718-P, IJCI-2014-19691 and RYC-2016-20506; City University of New York; National Science Foundation, Grant/Award Number: CNS-0855217, CNS-0958379, 747238, 167 and 15

Handling Editor: Evan Economo

Abstract

Aim: Understanding the drivers of speciation within islands is key to explain the high levels of invertebrate diversification and endemism often observed within islands. Here, we propose an insular topoclimate model for Quaternary diversification (ITQD), and test the general prediction that, within a radially eroded conical island, glacial climate conditions facilitate the divergence of populations within species across valleys.

Location: Gran Canaria, Canary Islands.

Taxon: The *Laparocerus tessellatus* beetle species complex (Coleoptera, Curculionidae).

Methods: We characterize individual-level genomic relationships using single nucleotide polymorphisms produced by double-digest restriction site associated DNA sequencing (ddRAD-seq). A range of parameter values were explored in order to filter our data. We assess individual relatedness, species boundaries, demographic history and spatial patterns of connectivity.

Results: The total number of ddRAD-seq loci per sample ranges from 4,576 to 512, with 11.12% and 4.84% of missing data respectively, depending on the filtering parameter combination. We consistently infer four genetically distinct ancestral populations and two presumed cases of admixture, one of which is largely restricted to high altitudes. Bayes factor delimitation support the hypothesis of four species, which is consistent with the four inferred ancestral gene pools. Landscape resistance analyses identified genomic relatedness among individuals in two out of the four inferred species to be best explained by annual precipitation during the last glacial maximum rather than geographic distance.

Main conclusions: Our data reveal a complex speciation history involving population isolation and admixture, with broad support for the ITQD model here proposed. We suggest that further studies are needed to test the generality of our model, and enrich our understanding of the evolutionary process in island invertebrates. Our results demonstrate the power of ddRAD-seq data to provide a detailed understanding of the temporal and spatial dynamics of insular biodiversity.

KEYWORDS

arthropod, dispersal, diversification, invertebrate, island biogeography, Pleistocene glaciation, Quaternary, species range

1 | INTRODUCTION

The study of invertebrate speciation on oceanic archipelagos has been the focus of much attention due to the well-defined geographic boundaries of individual islands, the typical historical geographic isolation of islands from each other (but see Rijsdijk et al., 2014), their dynamic and complex history of volcanism, and an often-strong endemic species component of their biodiversity. Molecular phylogenetic approaches have been an important source of information to understand both the tempo and geography of species origins in oceanic island settings (e.g. Contreras-Diaz, Moya, Oromi, & Juan, 2007; Dimitrov, Arnedo, & Ribera, 2008; Sequeira, Lanteri, Albelo, Bhattacharya, & Sijapati, 2008; Shapiro, Strazanac, & Roderick, 2006; Shaw & Gillespie, 2016), contributing to our understanding of patterns of community assembly and turnover (e.g. Emerson, 2003; Emerson & Gillespie, 2008; Emerson & Oromi, 2005). Population-level approaches have revealed the importance of colonization dynamics among islands in the speciation process, highlighting how repeated colonizations of an island and gene exchange among different populations and species among islands can play an important role in speciation (Hendrickx et al., 2015; Jordal, Emerson, & Hewitt, 2006). Population-level studies are informative about divergence, gene flow, establishment of reproductive isolation and speciation, and the factors that promote it. However, compared to phylogenetic analyses of speciation history, studies that specifically address the speciation process in invertebrates within oceanic islands are few. Thus, understanding the drivers of invertebrate speciation within islands, in particular the potential for interactions among geology, topography and climate to promote speciation by local geographic isolation, is a key challenge (Patiño et al., 2017).

It is increasingly recognized that Quaternary glacial cycles have impacted oceanic islands due to coincident sea-level and climate changes (e.g. Ali & Aitchison, 2014; Rijsdijk et al., 2014). Sea-level changes can cause substantial changes in island area, isolation and connectivity, now seen as consequential for patterns of island endemism across oceanic archipelagos and their underlying evolutionary dynamics (e.g. Norder et al., 2019; Papadopoulou & Knowles, 2015a, 2015b; Weigelt, Steinbauer, Cabral, & Kreft, 2016). At the archipelago scale, Gillespie and Roderick (2014) point out that such a dynamic can act as a "species pump", potentially facilitating isolation and speciation, with subsequent range expansions leading to sympatry in periods of higher connectivity. Within islands, transitions between glacial and interglacial climate conditions are also expected to alter the habitable area of organisms, typically through upslope and downslope shifts in species range limits. Fernández-Palacios et al. (2016) present a model describing how variation in Quaternary climatic factors must have enforced species elevational changes, further exaggerating isolation distances between islands caused by sea level changes alone during glacial conditions. While the implications for speciation between islands is obvious, there has been less focus on how Quaternary climate changes and their environmental consequences might impact speciation within islands.

The dynamic highlighted by Fernández-Palacios et al. (2016) raises interesting potential outcomes when considering topographically more complex islands. Using a conically shaped island as an example, Fernández-Palacios et al. (2016) illustrate how rising sea levels and upward-shifted climatic zones would simultaneously shift species distributions upslope and reduce their overall range size (Figure 1). The uniform topography considered by Fernández-Palacios et al. (2016) models expectations for a geologically young island, where erosional and catastrophic flank loss events are of minor consequence. In such a uniform landscape, climate is expected to change predictably with distance from the coast to the centre of the island. However, in older more eroded conical islands, spatial variation in local climate will be less uniform, and less predictable based on radial distance. The topographically complex conical island of Gran Canaria in the Canary Islands provides a useful example of this. Local climate station data has been used to demonstrate that pluviseasonal bioclimatic conditions are structured by variation in elevation and exposition (Figure 2), resulting in a complex matrix of climate discontinuity across the island (del-Arco, 2002).

Evidence has been provided for maximum levels of isolation among arthropod populations on different islands during present

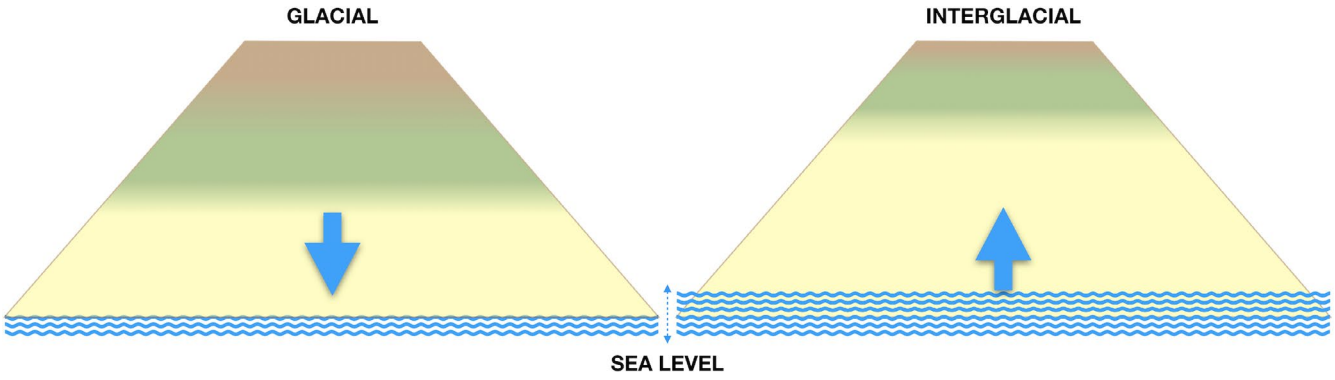

FIGURE 1 Quaternary climate change and oceanic island species distributions. Rising sea levels and upward-shifted climate zones during interglacial conditions are expected to impact upon the glacial distributions of individual species and habitats within oceanic islands. As climate transitions from glacial to interglacial conditions, a general tendency for upslope shifts is expected (modified from Fernández-Palacios et al., 2016)

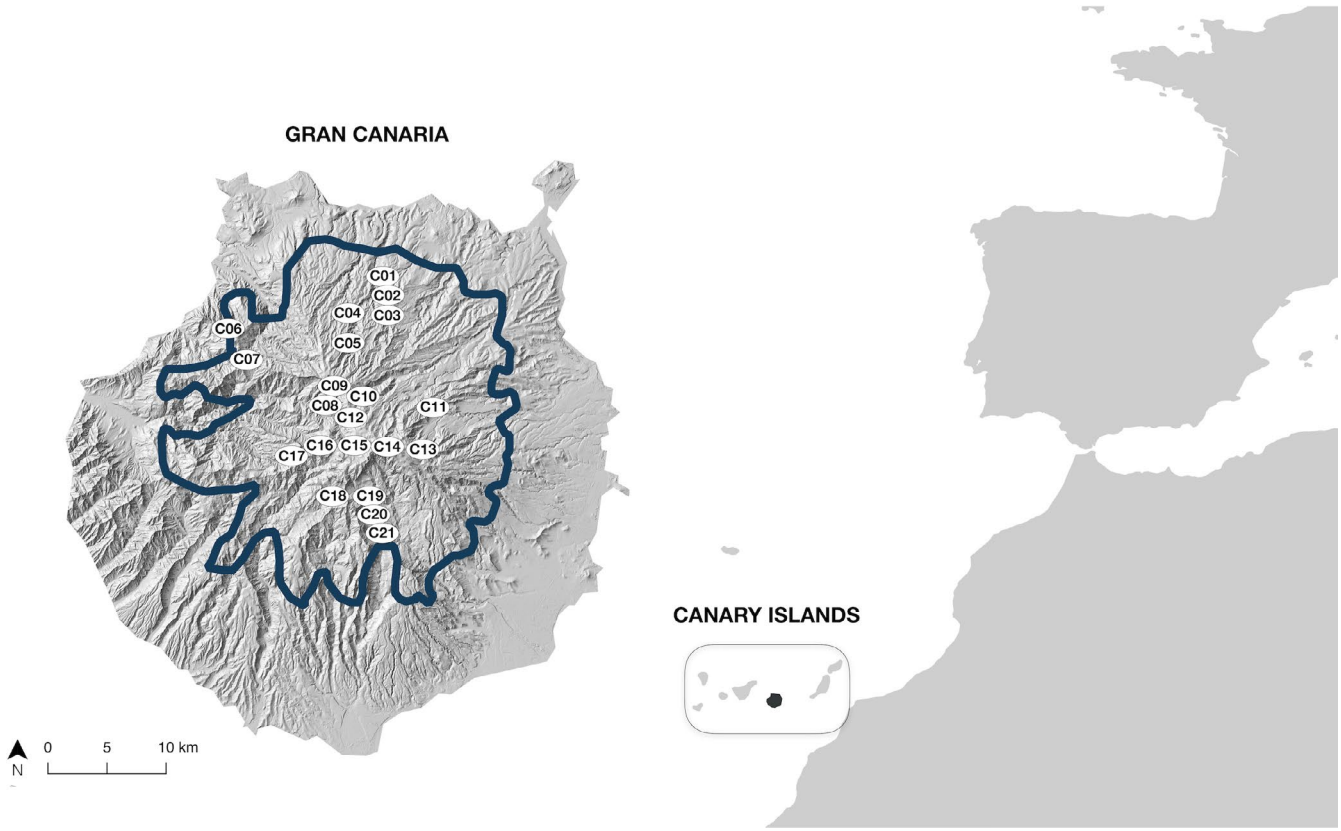

FIGURE 2 Sampling of the *Laparocerus tessellatus* complex in Gran Canaria. Map showing the location of the Canary Islands relative to Northwest Africa, and the geography of the archipelago with Gran Canaria highlighted in black. Sampling sites are shown within the island of Gran Canaria, together with the estimated distribution limits of the pluviseasonal bioclimate

day interglacial conditions (e.g. Jordan, Simon, Foote, & Englund, 2005; Papadopoulou & Knowles, 2015a, 2015b), providing some support for the hypothesized "species pump" action of rising and falling sea levels under the "Pleistocene Aggregate Island Complex" (PAIC) (Brown & Diesmos, 2002; Brown, Siler, Diesmos, & Alcala, 2009; Esselstyn & Brown, 2009; Heaney, 1985). We propose that Quaternary climate oscillations may have led to analogous changes in population connectivity, within islands, due to changes in the climate landscape. Dispersal limitation is a frequent feature of insular arthropods, and it has been recognized that together with landscape variation, such dispersal limitation can promote isolation and initiate speciation within islands (Goodman, Welter, & Roderick, 2012), even at relatively small geographic scales (Vandergast, Gillespie, & Roderick, 2004). Variation in climate across topographically complex islands, together with (a) climatically sensitive species with limited dispersal ability, and (b) cyclical alternation between glacial and interglacial conditions, could promote a dynamic of population divergence and coalescence within islands, with potentially profound population genetic and evolutionary consequences.

Here, we develop and test predictions for such a model which we refer to as an insular topoclimate model for Quaternary diversification (hereafter termed as ITQD). To explore this model, we use the geographic context of the eroded conical landscape of Gran Canaria. We propose that during temporally more persistent glacial conditions, species ranges would have extended down to their lowest elevations. At these low elevations species may have reached their broadest potential range sizes, but due to high topographic complexity at lower elevations, they may have also experienced the greatest potential for spatial isolation by climate within islands (Figure 3). As conditions transitioned from glacial to interglacial, distributions would have shifted to higher elevations and a simpler geographic climate matrix, something that should facilitate secondary contact among populations previously isolated at lower elevations (Figure 3). We evaluate predictions from the ITQD model using genomic data from a candidate system of dispersal limited beetles from the weevil genus *Laparocerus* on Gran Canaria. This is an ideal model system for a number of reasons related to both the biology of the focal group, the *Laparocerus tessellatus* species complex, and the radially eroded geology of the island of Gran Canaria.

The *L. tessellatus* complex comprises 10 taxonomically described species and an additional undescribed species distributed across four islands, with each species being a single island endemic. Species are dispersal limited and patchily distributed, with a clear association to local humidity (Machado & Aguiar, 2005). The five taxonomically recognized species within the topographically and climatically complex island of Gran Canaria, have ranges that

fall within the pluviseasonal bioclimate of the island (Figure 2). A recent phylogenetic analysis for the genus *Laparocerus* revealed speciation within islands to be an important driver for the diversification of the 196 taxonomically described species and subspecies in the Canary Islands (Machado, Rodriguez-Exposito, Lopez, & Hernandez, 2017). Recent population level analyses of closely related species within the *L. tessellatus* complex have further revealed less than simple patterns of individual relatedness among islands (Faria et al., 2016), subsequently explained by mega-landslides facilitating movement between islands involving multiple individuals (García-Olivares et al., 2017). However, there is less understanding about what factors have promoted divergence and speciation within islands, although Faria et al. (2016) present suggestive evidence for environmental barriers promoting both isolation and secondary contact.

Several recent DNA sequence-based analyses provide consistent evidence that Gran Canaria is the origin of the *L. tessellatus* complex. A Bayesian phylogenetic analysis concluded that the *L. tessellatus* complex belongs to a monophyletic group of potential subgenus status (Machado et al., 2017) that includes a further 21 species. All but three of the additional 21 species are endemic to Gran Canaria, consistent with a Gran Canarian origin for the complex. Faria et al. (2016) arrived to the same conclusion based on the geographic distribution of *ITS2* variation across the four islands of the complex, although mtDNA variation was less informative. However, increased mtDNA sampling and network analyses in García-Olivares et al. (2017) confirmed the inferred ancestral mtDNA haplotype for the complex to have a Gran Canarian origin. Gran Canaria is represented by four taxonomically described species from the *L. tessellatus* complex: *L. microphthalmus* Lindberg, 1950; *L. obsitus* Wollaston, 1864; *L. osorio* Machado, 2012; and *L. tirajana* Machado, 2012. However, there are inconsistencies between these taxonomic entities and relationships inferred from both mtDNA and nuclear sequence data (see Faria et al., 2016 for details), highlighting the need for different sequencing technologies that can increase resolution in order to infer the recent diversification history of the *L. tessellatus* complex. Due to their potential to yield data from thousands of loci, reduced representation genome sequencing approaches offer the opportunity to quantify individual relatedness and population genetic structure with as few as two individuals per population (Nazareno, Bemmels, Dick, & Lohmann, 2017). Here, we apply double-digest restriction site associated DNA sequencing (ddRAD-seq; Peterson, Weber, Kay, Fisher, & Hoekstra, 2012) to investigate in more detail evolutionary process within the *L. tessellatus* species complex.

The onset of the relative volcanic quiescence within the island of Gran Canaria *c.* 3 Ma, known as the post-Roque Nublo period, predates estimates for the initiation of diversification within the *L. tessellatus* complex. Applying a general coleopteran COII mutation rate to mtDNA sequence variation within the complex, Faria et al. (2016) estimated the onset of diversification to have been *c.* 2.7 Ma. More recently, Machado et al. (2017) used geological age constraints to calibrate their tree with a more complete sampling of the genus *Laparocerus*, and estimated the age of onset to be *c.* 1.24 Ma. Thus, diversification falls within a period where volcanic activity has been characterized by localized low intensity activity in Gran Canaria, providing an opportunity to investigate diversification within a landscape subjected to the more subtle changes of millennial-scale erosional activity and climate variation.

In the present study, we first describe patterns of genomic relatedness among individuals, and then test the fit of competing hypotheses for species boundaries derived from taxonomy and RAD-seq data. We then use the best fit species model to test the following three predictions from our ITQD model, in the context of a radially eroded conical island. Prediction 1 is that transitory interglacial conditions favour high elevation secondary contact and potential gene flow between species or populations that were previously isolated at lower altitudes during glacial conditions (Figure 3). Evidence for this prediction would be provided by signatures of admixture among species or populations at higher elevations. The more obvious potential mechanism for speciation within a topoclimate model would be through increased bioclimate fragmentation during glacial conditions, together with the colonization of new favourable bioclimatic areas mediated by higher bioclimate connectivity during interglacial conditions (Figure 3). Following from this, prediction 2 is that there would be lower genetic distance (higher genetic connectivity) among populations along altitudinal transects (i.e. down ridges and valleys), and higher genetic distance across radial transects (i.e. across ridges and valleys). A third prediction, derived from the expected higher genetic connectivity under interglacial conditions, is that populations should present signatures for demographic expansion consistent with the transition from glacial to interglacial conditions.

2 | MATERIALS AND METHODS

2.1 | Geological context of Gran Canaria

Gran Canaria is located at the centre of the Canarian archipelago with a maximum elevation of 1,950 m above sea level, and geologically it is likely one of the most comprehensively studied oceanic islands in the world (Carracedo & Troll, 2016). The geology of Gran Canaria can be broadly summarized as first involving a juvenile or shield forming stage (from 14.5–8.0 Ma), which includes basaltic shield growth on the submarine seamount, followed by a period of volcanic inactivity, and finally a stage involving renewed activity from 5.5 Ma to the present. This last stage is divided into two eruptive periods: Roque Nublo stratovolcanism and Post-Roque Nublo volcanism (Aulinas et al., 2010; Carracedo & Day, 2002; Guillou, Torrado, Hansen Machin, Carracedo, & Gimeno, 2004; Pérez-Torrado, Carracedo, & Mangas, 1995). Since the end of the Roque Nublo eruptive period, *c.* 3 Ma, Gran Canaria has been relatively inactive in terms of volcanic activity, characterized by local explosions related to hydromagmatic deposits (Anguita, Márquez, Castiñeiras, & Hernán, 2002), fissures and small-size monogenetic centers (Karátson, Yepes, Favalli, Rodríguez-Peces, & Fornaciai, 2016), with more recent activity limited to the north-northeast of the island (Rodriguez-Gonzalez et al., 2012).

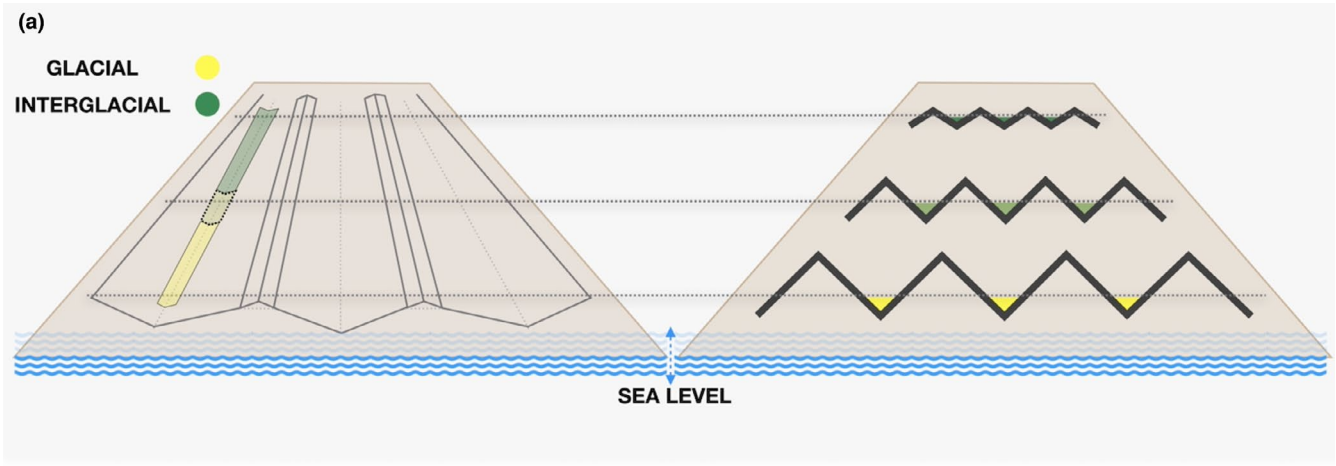
(a)
GLACIAL
INTERGLACIAL
SEA LEVEL

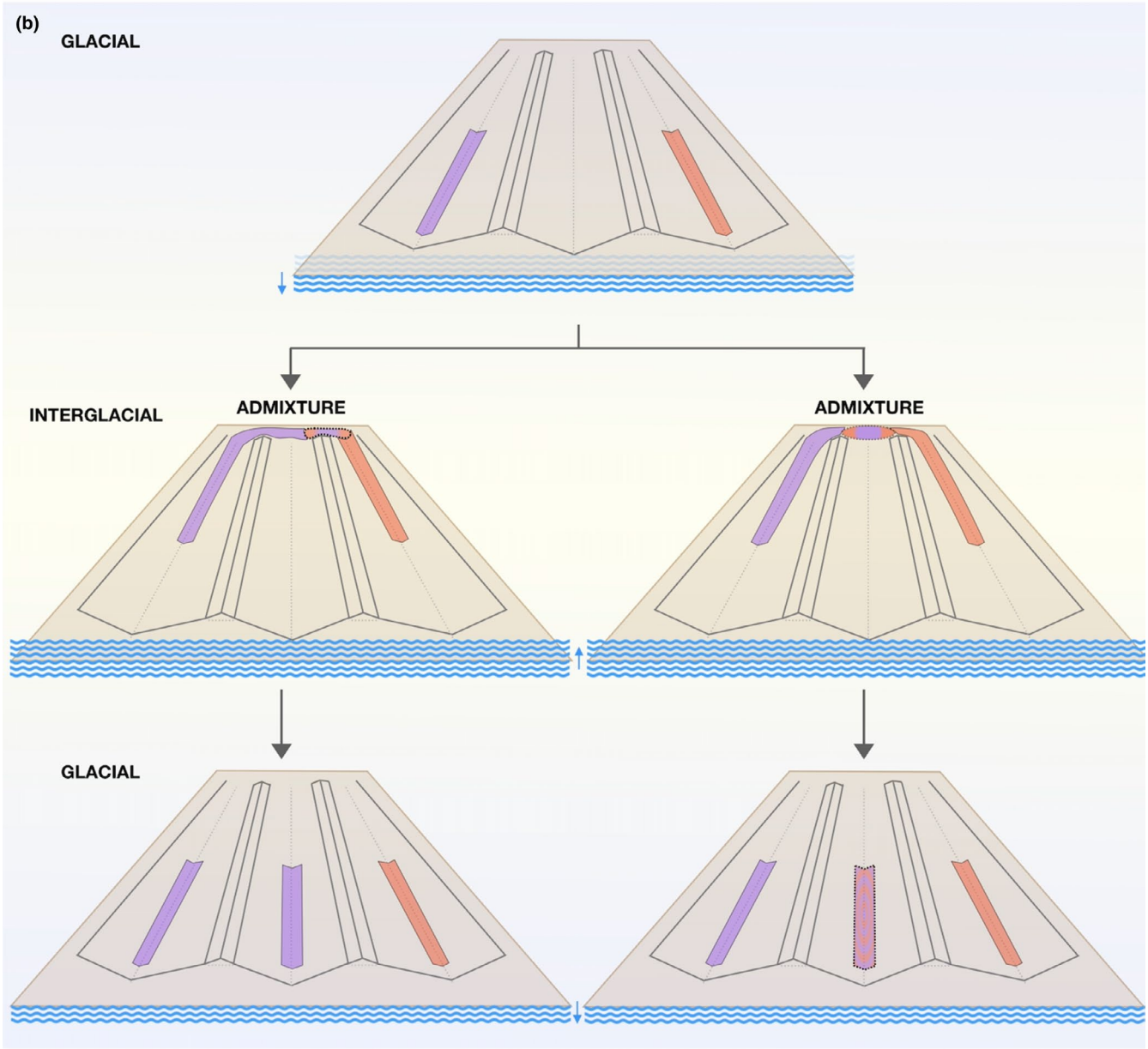
(b)
GLACIAL
INTERGLACIAL
ADMIXTURE
ADMIXTURE
GLACIAL

FIGURE 3 An insular topoclimate model for Quaternary diversification (ITQD). (a) A simplified island model is shown in the left panel, where topography is marked by erosional activity and the formation of valleys. Hypothetical species distributions are depicted as polygons representing range limits during glacial and interglacial climate conditions. Yellow represents interglacial conditions, when sea levels are at their lowest and global climate conditions at their coolest. Green represents range limits during warmer interglacial conditions, with overlap between glacial and interglacial ranges denote with an intermediate colour. The right panel represents isolation by bioclimate across valleys at different altitudes. In this example, a species with favourable climate associated with valley floors experiences reduced isolation by environment at higher elevations where the amplitude of topographic separation among valleys is reduced. (b) Two potential outcomes of glacial-scale climate change for two species (purple and red) distributed in different valleys during glacial climate conditions (top panel). During the transition from glacial to interglacial climate conditions, rising sea-level and upward-shifted climate zones result in upslope shifts in the distribution limits of both species, with contact and admixture in high elevation areas of low topographic complexity (middle panel). As climate transitions back to glacial conditions, species range limits shift downslope, potentially facilitating the colonization of a new valley by parental species (bottom panel, left), or even by new admixed populations (bottom panel, right)

2.2 | Sample collection and sample selection

Representative geographical sampling for the Gran Canarian species of the *L. tessellatus* complex was achieved by complementing the 10 sampling sites of Faria et al. (2016) with samples from 11 new sites. For each taxonomic species an average of three individuals from each sampling site were sequenced for a region of the mitochondrial COII gene. This was done to identify potential sites of sympatry for the two divergent mtDNA clades described by Faria et al. (2016) and García-Olivares et al. (2017), facilitating direct testing of their association with species boundaries. DNA was extracted using a Chelex extraction protocol (Casquet, Thebaud, & Gillespie, 2012) using two hind legs. PCR amplifications were performed using conditions described in Faria et al. (2016) and sequenced with the Sanger DNA sequencing service of Macrogen (www.macrogen.com). Sequences were edited with GENEIOUS R10.2.2 (http://geneious.com, Kearse et al., 2012) and aligned with sequences from Faria et al. (2016) using MAFFT 6.814 (Katoh, Misawa, Kuma, & Miyata, 2002). A Bayesian tree was then constructed using MRBAYES 3.2.6 (Ronquist et al., 2012), applying the same parameters described in Faria et al. (2016). Four analyses were performed, each with 100 million generations using four Markov chain Monte Carlo (MCMC) chains, and sampling trees every 1,000 generations, using *L. vicinus* as an outgroup. TRACER 1.6 (Rambaut, Drummond, Xie, Baele, & Suchard, 2018) was used to confirm that the average standard deviation of split frequencies was below 0.01 at the completion of the analysis; and to verify that effective sample size (ESS) values were above 200. Trees were visualized in FIGTREE 1.4.2 (Rambaut & Drummond, 2014).

2.3 | RAD-seq library preparation

For each taxonomic species two individuals from each sampling site were selected for RAD-sequencing. Based on the results of the mtDNA sequencing, several additional samples were included to represent divergent mtDNA lineages sampled in sympatry. DNA extractions were performed using the Qiagen DNeasy Blood & Tissue kit following the manufacturer's instructions. A total of 51 individuals from the *L. tessellatus* complex were analysed following modifications of the protocol of Mastretta-Yanes et al. (2015). Full details of the protocol are included in Appendix S1. After DNA extraction, digestion was performed using the enzymes EcoRI and MseI. Individuals from Gran Canaria were analysed together with a total of 224 individuals representing the remaining species of the complex from the western islands of the archipelago. In the light of complex patterns of mtDNA relatedness among individuals from Gran Canaria and other islands (Faria et al., 2016; García-Olivares et al., 2017), non-Gran Canaria samples were used to first assess relatedness among individuals of the complex from Gran Canaria and other islands. A total of 48 samples (including 11 individuals from Gran Canaria, four replicates and two negative controls) were first sequenced, randomly assigning samples to one of two sequencing indexes (ddRAD libraries hereafter). Both ddRAD libraries were pooled at equimolar ratios and size selected for fragments between 200–250 bp, and then sequenced using single-end reads (100 bp long) in a single lane of an Illumina HiSeq2500 (Lausanne Genomic Technologies Facility, University of Lausanne, Switzerland). Based upon the mean depth from these first two libraries, a further 234 individuals were sequenced across three lanes (78 individuals, plus 1 replicate and 1 negative control). Samples within each lane were randomly assigned to one of four libraries for each (3 libraries with 24 samples, 1 library with 8 samples).

2.4 | Bioinformatic and population genomic analysis

RAD-seq data were demultiplexed, quality filtered and de novo clustered using IPYRAD 0.7.19 (Eaton & Overcast, 2016). Only reads with unambiguous barcodes and fewer than five low quality bases (Phred quality score < 20), were retained, and a strict filter was applied to remove Illumina adapter contaminants. A first analysis was undertaken with all 273 individuals to assess patterns of relatedness among individuals of the complex from Gran Canaria and other islands. For this analysis, parameters were arbitrarily set to the following values: clust_threshold (the sequence similarity threshold) = 0.87, max_SNPs_locus (the maximum number of SNPs allowed in a locus) = 20, and min_samples_locus (the minimum number of samples that must have data at a given locus for that locus to be retained in the final data set) = 60%, with all remaining parameter values set to their default values.

To identify optimal parameter values for the analysis of individuals from Gran Canaria, a range of parameter values were explored for clust_threshold (0.85, 0.87, 0.90 and 0.93), max_SNPs_locus (5, 10, 15, 20, 40) and min_samples_locus (40%, 60%, 80% and 90%),

with all remaining parameter values set to their default values, yielding a total of 80 different combinations. Outputs from each analysis were processed using VCFTOOLS (Danecek et al., 2011) to calculate: (a) total number of loci, (b) the distribution of SNPs across loci, (c) mean depth, and (d) missing data. Results from the 80 parameter combinations were used to evaluate the effect of each parameter on the number of loci recovered as (a) the parameter value varies in a background of fixed values for other parameters and (b) as other parameter values are varied while the parameter of interest remains constant. These observations were then used to (a) identify and exclude parameter values that indicate assembly problems, and then (b) identify parameter combinations that yield a high number of loci.

We then evaluated the congruence of signal between the parameter combination yielding the highest number of loci, which we refer to as a "relaxed" combination, and the most "conservative" parameter combination. To evaluate congruence between both parameter combinations we used principal component analysis (PCA) to describe the existence of groups of individuals and sNMF cross-entropy to compare the number of inferred ancestral populations, and individual ancestry coefficients. PCA analyses were performed using ADEGENET 2.1.0 package (Jombart & Ahmed, 2011) and sNMF using the LEA package (Eric Frichot, François, & O'Meara, 2015) in R 3.4.2 (R Core Team 2013). The sNMF algorithm provides least-squares estimates of ancestry proportions to infer individual ancestry and population clustering (Frichot, Mathieu, Trouillon, Bouchard, & Francois, 2014). To obtain the best-fit number of ancestral populations (*K*) within Gran Canaria, *K* values from 1–10 were evaluated with 1,000 replicates per K, using a cross-entropy criterion to identify the best fit value of K. Congruence between relaxed and conservative parameter combinations was accepted if the same groups are represented by PCA, and the same number and composition of ancestral populations were inferred by sNMF. In the absence of congruence stricter parameter combinations were evaluated until congruence with the relaxed parameter combinations was obtained. Upon identifying an appropriate parameter combination, replicate samples were used to estimate genotyping error (Mastretta-Yanes et al., 2015).

2.5 | Species delimitation

The Bayes factor delimitation (BFD) approach (Leache, Fujita, Minin, & Bouckaert, 2014) was implemented to evaluate competing species delimitation hypotheses, derived from taxonomy and RAD-seq data, using SNAPP (Bryant, Bouckaert, Felsenstein, Rosenberg, & RoyChoudhury, 2012). This approach uses an explicit multispecies coalescent (MSC) framework to calculate and compare marginal likelihood estimates (MLE) for alternative species delimitation hypotheses. While SNAPP is able to accommodate lineage sorting, it assumes that there is no gene flow between taxa (Bryant et al., 2012). Thus, prior to the BFD analyses individuals with more than 10% assignment to an alternative ancestral population were considered admixed (Jombart & Collins, 2015) and removed from the data set. These individuals were subsequently assessed for potential hybrid origin (see following section). A path sampling analysis with 14 steps and an a-value of 0.3 with 100,000 MCMC generations and a pre burn-in of 10% was used.

2.6 | Evaluating admixed individuals

Individuals identified as being of presumed admixed origin from sNMF and PCA analyses were further assessed using HYBRIDLAB (Nielsen, Bach, & Kotlicki, 2006). The data set was filtered using VCFTOOLS, to generate data sets comprising individuals of presumed admixed origin and their inferred parental populations. The set of recovered loci was then filtered for those loci presenting an F_{ST} estimate falling between 0.8 and 1.0 between parental populations. Selected loci were then used to simulate the following crosses: F1, F1 backcross with parent 1, F1 backcross to parent 2, F2. Simulated genotypes were then plotted to represent ancestry assignment and heterozygosity, together with estimates for parental and individuals of presumed admixed origin, using the GRAPHICS package in R 3.4.2.

2.7 | Landscape patterns of genomic similarity and demography

To explore patterns of genetic distance among sampling sites within species inferred with BFD, the Neighbor-Net algorithm in SPLITSTREE 4.14.5 (Huson & Bryant, 2006) was used to summarize individual genomic relatedness, sampling a single SNP from each locus. Edge weights from splits graphs provide a measure of relatedness among nodes, facilitating their use as a proxy of genetic connectivity when nodes represent sampling sites and graphs are constructed from multiple genetic loci. By analysing a smaller number of more related individuals within species, more loci are expected to be recovered in the assembly process. Thus, to optimize the recovery of informative loci, individual species were processed with IPYRAD using the previously identified optimal parameter combination. To quantify differences in genetic distance among sampling sites, 100 bootstrap replicates were sampled from empirical SNP matrices and used to generate bootstrapped distributions for edge weights, which were corrected by geographic distance. Transformed edge weights were then used to generate mean bootstrapped edge weights and to test for significant differences between pairs of sampling sites using a non-parametric Kruskal–Wallis test followed by a Nemenyi-test for multiple comparisons of (mean) rank sums of independent samples; both tests were performed in R 3.4.2 (R Core Team 2013).

To test for signatures of recent demographic expansion under the assumption of selective neutrality, we used Tajima's *D* (Tajima, 1989) and Fu and Li's *D* (Fu & Li, 1993) neutrality tests conducted in DNASP 6 (Rozas et al., 2017), using all SNPs. While some loci may be under selection, it is not unreasonable to assume that the great majority are behaving neutrally. Significantly negative values for Tajima's *D* and Fu and Li's *D* point to an excess of rare polymorphisms in a given population, which can be an indication of a recent increase in population size. In contrast, significantly positive values indicate a recent population contraction.

2.8 | Landscape resistance analyses and isolation by distance

In order to make mechanistic inferences about what factor(s) could best explain geographic patterns of genetic structure within the *L. tessellatus* complex, we tested among alternative hypotheses, including isolation by distance, topographic-mediated isolation, and historical (glacial) and recent (interglacial) climate-driven isolation. To do this we used the R package ResistanceGA 4.0 (Peterman, 2018) which both optimizes and selects resistance surfaces to optimally fit genetic data. This approach circumvents typical issues such as spatial autocorrelation and high dimensionality that resistance surfaces can have, and subjectivity in assigning resistance values (Peterman, 2018; Peterman, Connette, Keitt, & Shah, 2014). Pairwise genomic distances between individuals, estimated following the approach proposed by Petkova, Novembre, and Stephens (2015), were used as the dependent variable, while scaled and centred circuit resistance distance matrices between individuals were used as independent variables. Analyses were applied to inferred species and admixed individuals assigned to them (see population genomic analyses). For each species analysed, two data treatments were used: the first treatment included all individuals, while the second treatment excluded admixed individuals.

To calculate pairwise resistance distances between individuals, we used the random-walk commute time algorithm (function "commuteDistance" in "gdistance"), a genetic algorithm to maximize fit of resistance surfaces similar to CIRCUITSCAPE (McRae, 2006; McRae, Dickson, Keitt, & Shah, 2008). We used the wrapper function "all_comb" in ResistanceGA to implement single-surface and multiple-surface optimization, followed by a bootstrapping step. For the multiple-surface optimization, we simultaneously combined two or three resistance surfaces to optimize and create a novel composite resistance surface. Mixed models were fitted using the maximum-likelihood population effects (MLPE) parameterization implemented in the R package LME4 (Bates, Maechler, Bolker, & Walker, 2014), as proposed in Peterman (2018) and Peterman et al. (2014).

We assessed the influence of eight climatic and topographic variables on genomic relatedness among individuals. These variables are expected to have some functional relationship to water stress or geographic isolation, and include (a) contemporary mean annual precipitation; (b) mean annual precipitation at the Last Glacial Maximum (LGM); (c) contemporary mean annual temperature; (d) mean annual temperature at the LGM (Karger et al., 2017); (e) a digital elevation model (DEM; Danielson & Gesch, 2011); and three topographic indexes estimated from the DEM layer in SAGA QGIS, including (f) position index (TPI), (g) ruggedness index (TRI) and (h) wetness index (TWI). TPI is a measure which compares the elevation of each cell with the mean elevation of a specified neighbourhood around that cell, TRI describes the amount of elevation difference between adjacent cells of a digital elevation grid, and TWI quantifies topographic control on hydrological processes. All layers had a spatial resolution of 1 km × 1 km. In addition to the climatic and topographic resistance surfaces, we assessed Euclidean distance alone (isolation by distance) as well as an intercept only null model.

3 | RESULTS

3.1 | Bioinformatic analyses

In contrast with the mtDNA results of Faria et al. (2016) and García-Olivares et al. (2017), nuclear genomic data revealed a simpler pattern of relatedness between individuals from Gran Canaria and other islands. A preliminary PCA using all 275 individuals from across all islands (Figure S2.1 in Appendix S2) revealed individuals from Gran Canaria to form a cluster, being clearly distinct from other islands. Thus, for subsequent analyses only individuals from Gran Canaria were analysed. From this data set two individuals were removed, one with a low number of reads and the other due to a high level of missing data (more than 30%).

A total of 178.37 million reads were sequenced for the data set from Gran Canaria, of which 169.85 million reads passed the quality filtering steps of IPYRAD. Per sample an average of 3.46 (±1.58 *SD*) million reads were recovered. Results from the optimization step are summarized in Figure S2.2 in Appendix S2. Lower values for min_samples_locus resulted in the recovery of more loci across the 80 parameter combinations explored within IPYRAD for genotype assembly. However, a trend towards a decreasing number of recovered loci was observed at values of 40% and 60% as the value of clust_threshold was reduced, at a given value for max_SNPs_locus, being more pronounced for lower values of max_SNPs_locus. This counterintuitive trend suggests that at lower values for min_samples_locus, divergent alleles may be excluded during clustering, allowing for the partial assembly of loci across a subset of individuals presenting a subset of less divergent alleles. Thus, while lower values of min_samples_locus may be appealing for the larger number of loci they can potentially retrieve, we chose to avoid such parameter combinations (i.e. those with min_samples_locus of 40% and 60%) due to concerns that they may increase genotyping error. In contrast, the number of recovered loci increased as clust_threshold was reduced for values of 80% and 90% for min_samples_locus, consistent with the expectation that, for a given value of max_SNPs_locus, as clust_threshold is decreased, loci with more divergent alleles are assembled.

From the remainder of the sensitivity analyses including min_samples_locus = 80% or 90%, the parameter combination yielding the highest number of loci was as follows: clust_threshold = 0.85, max_SNPs_locus = 40, min_samples_locus = 80%, yielding a total of 4,576 (±228.14 *SD*) loci per sample, with 11.12% of missing data. In contrast with this relaxed parameter combination, the most conservative parameter combination (clust_threshold = 0.93, max_SNPs_locus = 5, min_sample_locus = 90%) yielded an average of 512 (±19.98 *SD*) loci per sample with 4.84% of missing data. Locus and allele error rates were calculated using the sample replicate approach of Mastretta-Yanes et al. (2015) for the relaxed parameter combination revealing error rates of 0.029 and 0.002, respectively.

3.2 | Population genomic analyses

A comparison of inferences derived from both the sNMF and PCA analyses for both the relaxed and conservative parameter

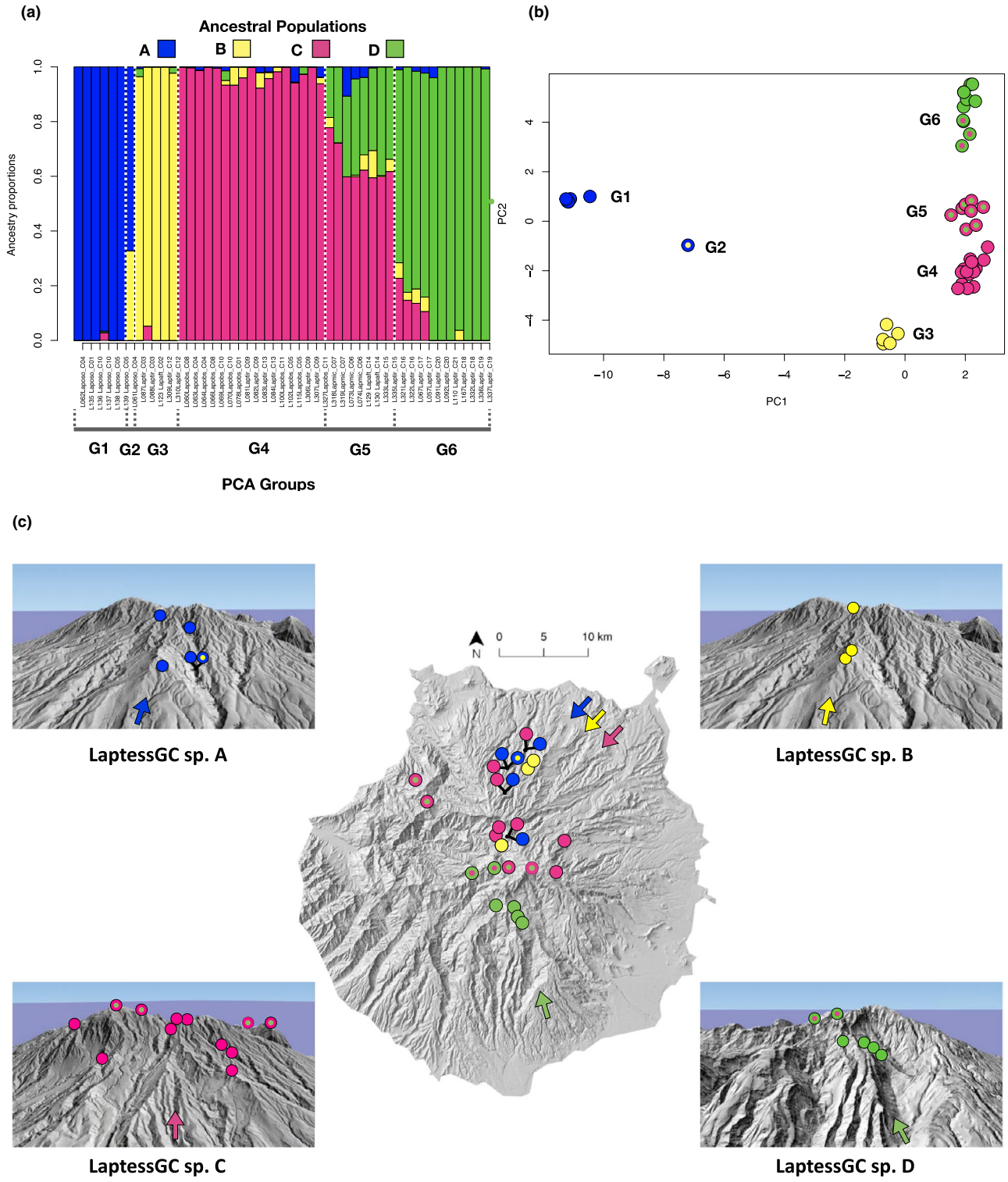

FIGURE 4 Ancestry assignment and individual clustering in the *Laparocerus tessellatus* complex using genotypes derived from assembly with the relaxed parameter combination. (a) sNMF assignment of individual ancestry to ancestral populations A, B, C and D. Individuals are grouped with respect to PCA clustering (see 4b). (b) Principal component analysis (PCA) of multilocus genotypes for individuals. Each point represents one individual, with colours corresponding to inferences of ancestry assignment with sNMF in (a). Individuals inferred to be of mixed ancestry with sNMF (more than 10% of the genome inferred to be from a second ancestral population) are represented with a coloured dot representing the minor representation genome. (c) Sampling sites are represented by circles and are colour coded with respect to probable genomic clusters identified by PCA (b). Black lines indicate sampling sites when more than one genomic cluster was sampled at a site. All sampling sites are represented in the central map. Sampled distributions of each of the four species inferred by Bayes factor delimitation are shown using 3D digital terrain models, with orientation relative to the central map indicated with coloured arrows. Sites with admixed individuals are represented on the terrain model of the parental species with the higher contribution to the admixed genome

combinations for genotype assembly in IPYRAD revealed congruence. The cross-entropy criterion identified four ancestral populations for both the relaxed (Figure 4a) and conservative (Figure S2.3a) data sets, with consistent individual assignments inferred across both analyses. The relaxed parameter combination described six PCA groups with all but two groups (G4 and G5) showing clear separation (Figure 4b). Genotype data assembled from the conservative parameter combination described four PCA groups (Figure S2.3b), three of which are described in Figure 4b (G1, G2, G3), with the fourth comprising the remaining groups in Figure 4b (G4, G5, G6). Comparing inferences from the sNMF ancestry coefficients and PCA analysis (Figure 4), there is clear correspondence between both. PCA groups G1, G3 and G4 are exclusively comprised of all individuals assigned with high probability (>90%; see Table S2.1) to ancestral populations A, B and C, respectively. PCA group G6 includes all individuals assigned with high ancestry to ancestral population D, but also includes four individuals with from 13% to 23% assignment to ancestral population C (Table S2.1). The single individual comprising PCA group G2 is estimated to have shared ancestry between populations A and B, consistent with its intermediate position between G1 and G3 in the PCA. Finally, PCA group G5 comprises eight individuals with shared ancestry between populations C and D, consistent with the intermediate location of G5 between G4 and G6 in the PCA. *Laparocerus osorio* was the only taxonomically described species where all individuals were assigned to a single nuclear genomic population (A), to which no individuals from other taxonomic species were assigned. All but one individual of *L. osorio* was assigned with high probability to population A (PCA group G1), with the single exception also being assigned with 33% probability to population B (PCA group G2). The remaining taxonomic species did not segregate with nuclear data, with species either assigned to multiple populations, or to populations to which other species were also assigned, or both (Table S2.1). No correspondence was found between patterns of nuclear genotype relatedness and the two mtDNA lineages described by Faria et al. (2016) and García-Olivares et al. (2017), with sympatric divergent mtDNA lineages associating with highly related nuclear genotypes.

3.3 | Species delimitation

We identified seven initial competing species hypotheses derived from taxonomy and the population genomic analyses of RAD-seq data (Table 1). All samples from PCA groups G2 and G5, as well as four individuals from G6 were removed from the data set for SNAPP analyses because they presented signatures of admixture (i.e. more than 10% assignment to a second ancestral population). Removing these individuals reduced the final number of competing species hypotheses to four (Table 1). Bayes factor delimitation revealed highest support for hypothesis 3 (Table 1), in which four species are hypothesized (Figure 4c) based on sNMF and PCA separation of the four inferred ancestral gene pools. The correspondences of inferred species with respect to the sNMF ancestral populations (Figure 4a) and PCA groups (Figure 4b) are as follows: LaptessGC sp. A (G1), LaptessGC sp. B (G3), LaptessGC sp. C (G4) and LaptessGC sp. D (G6 without admixed individuals).

3.4 | Admixture

Two cases of presumed admixture were identified. In the first case a single individual comprising G2 (Figure 4a) was inferred to be of admixed origin between LaptessGC sp. A and LaptessGC sp. B. A total of 777 loci were identified as yielding an F_{ST} between 0.8 and 1 between LaptessGC sp. A and LaptessGC sp. B, providing strong diagnosability for first generation, second generation, or an older hybrid origin using HYBRIDLAB (Figure 5a). These results clearly identify the G2 individual as being derived from an older admixture event between LaptessGC sp. A and LaptessGC sp. B. While the data does not allow us to say how far back in the past, the fact that only one of the parental species (LaptessGC sp. A) was sampled together with G2 suggests ancient rather than recent admixture. The sympatric sampling of G2 together with both LaptessGC sp. A and LaptessGC sp. C (Figure 4c), with no signature of introgression, is consistent with reproductive isolation, and thus potential species status for G2. However, further sampling will be required to more rigorously assess the extent to which historical admixture between two morphologically distinct species, taxonomically assigned to the larger *L. osorio* and the smaller *L. tirajana*, has given rise to a new species that is morphologically cryptic with regard to *L. osorio*.

In the second case of inferred admixture, 12 individuals were inferred to be of admixed origin between LaptessGC sp. C and LaptessGC sp. D. The limited genetic differentiation between LaptessGC sp. C and LaptessGC sp. D resulted in only 26 loci with an F_{ST} between 0.8 and 1, providing only limited diagnosability of expected first and second-generation hybrid crosses (Figure 5b). All 12 individuals were identified as derived from admixture older than F1, with several individuals providing strong signatures of an admixed origin going back multiple generations. It is interesting to note that individuals from the same sampling site tend to share similar values of heterozygosity and ancestry. This, together with PCA inferences that relatedness among admixed individuals is geographically structured (Figure S2.4), and the absence of parental genotypes within any of the six sites with admixed individuals, suggests one or more admixture events of some antiquity.

3.5 | Genomic distance and demographic signal

Of the four species inferred by BFD in SNAPP, LaptessGC sp. A and LaptessGC sp. B present geographically proximate distributions down the northern slopes of the island, with each showing greater separation among populations along an altitudinal axis relative to a radial axis (Figure 4c). LaptessGC sp. D has a narrow distribution at higher altitudes of the southern slopes of the island (Figure 4c). The species with the broadest distribution is LaptessGC sp. C (Figure 4c). With a northern slope range that overlaps with LaptessGC sp. A, and further populations across the eastern slopes of the island, LaptessGC sp. C allows for the testing of higher genetic connectivity along altitudinal transects

compared to radial transects. A SPLITSTREE representation of relatedness within LaptessGC sp. C reveals high separation among individuals, but lower genetic distance among individuals from the same sampling site, with the exception of sites C08 and C09, separated by a distance of <700 m (Figure 6a). However, at a spatial separation from C08 and C09 of *c.* 1.3 km, the two individuals from C10 are clearly differentiated (Figure 6a). Distributions of bootstrapped edge lengths were generated from a data matrix representing each site with a single individual, collapsing C08 and C09 into a single site. Distributions were then used to calculate mean edge weight between sites capturing range limits, showing that values of genetic distance were significantly lower along altitudinal than across radial transects (Figure 6b). Tajima's *D* and Fu and Li's *D* were non-significantly negative ($p > .10$) in all cases, with the exception of LaptessGC sp. D, which was non-significantly positive (Table 2).

3.6 | Landscape resistance analyses

Landscape resistance analyses for LaptessGC sp. A identified genomic relatedness among individuals to be best explained by either geographic distance or a null model, while for LaptessGC sp. B geographic distance was identified as the model of best fit (Table 3). In contrast, for LaptessGC sp. C and LaptessGC sp. D, both of which presented individuals of admixed origin with the other species at higher elevations, genomic relatedness among individuals within each species was best explained by a single optimal model derived from landscape variation for annual precipitation during the LGM (Table 3). Landscape variation for annual precipitation during the LGM continued to be the single optimal model for LaptessGC sp. C even when admixed individuals were excluded, while for LaptessGC sp. D individual relatedness after removing admixed individuals was best explained by a null model (Table 3), although with a very low R^2 value. Importantly, for all three analyses of LaptessGC sp. C and LaptessGC sp. D where landscape variation in precipitation during the LGM best explained genomic relatedness among individuals, a model derived from geographic distance was a substantially poorer fit, as measured by ΔAICc (Table 3).

4 | DISCUSSION

While the interaction between topography and climate across glacial cycles has been recognized as a driver of diversification in continental

TABLE 1 Bayes factor delimitation. Results of the Bayes factor delimitation analyses to test for the best support among competing species delimitation hypotheses (H) within the *Laparocerus tessellatus* complex in Gran Canaria. Initial hypotheses are refined to final hypotheses after the exclusion of admixed individuals. For each model, the marginal likelihood estimate (MLE), Bayes factor (BF) and rank are shown. The best fit model is highlighted in bold

Initial hypotheses	Motivation	Groups	Final hypotheses	MLE	BF	Rank
H_a	Two major morphological groups	(G1, G2) (G3, G4, G5, G6)	H_1 two species (G1) (G3, G4, G6)	−39,818.0	2,206.3	4
H_b	Three groups described by PC1 (PCA with conservative parameters)	(G1) (G2) (G3, G4, G5, G6)				
H_c	Four taxonomic species (*L. osorio*, *L.microphthalmus*, *L. obsitus*, *L. tirajana*)	(G1, G2) (G4) (G5) (G3, G4, G5, G6)	H_2 three species (G1) (G4) (G3, G4, G6)	−40,357.0	2,745.3	3
H_d	**Five groups described by PC1 and PC2 (PCA with conservative parameters)**	**(G1) (G2) (G3) (G4, G5) (G6)**	**H_3 four species (G1) (G3) (G4) (G6)**	**−37,611.7**	–	**1**
H_e	**Six groups described by PC1 and PC2 (PCA with relaxed parameters)**	**(G1) (G2) (G3) (G4) (G5) (G6)**				
H_f	**Four groups described by sNMF (both conservative and relaxed parameter combinations)**	**(G1, G2) (G3) (G4, G5) (G6)**				
H_g	Four groups described by PC1 (PCA with relaxed parameters)	(G1) (G2) (G3) (G4, G5, G6)	H_4 three species (G1) (G3) (G4, G6)	−38,221.1	609.3	2

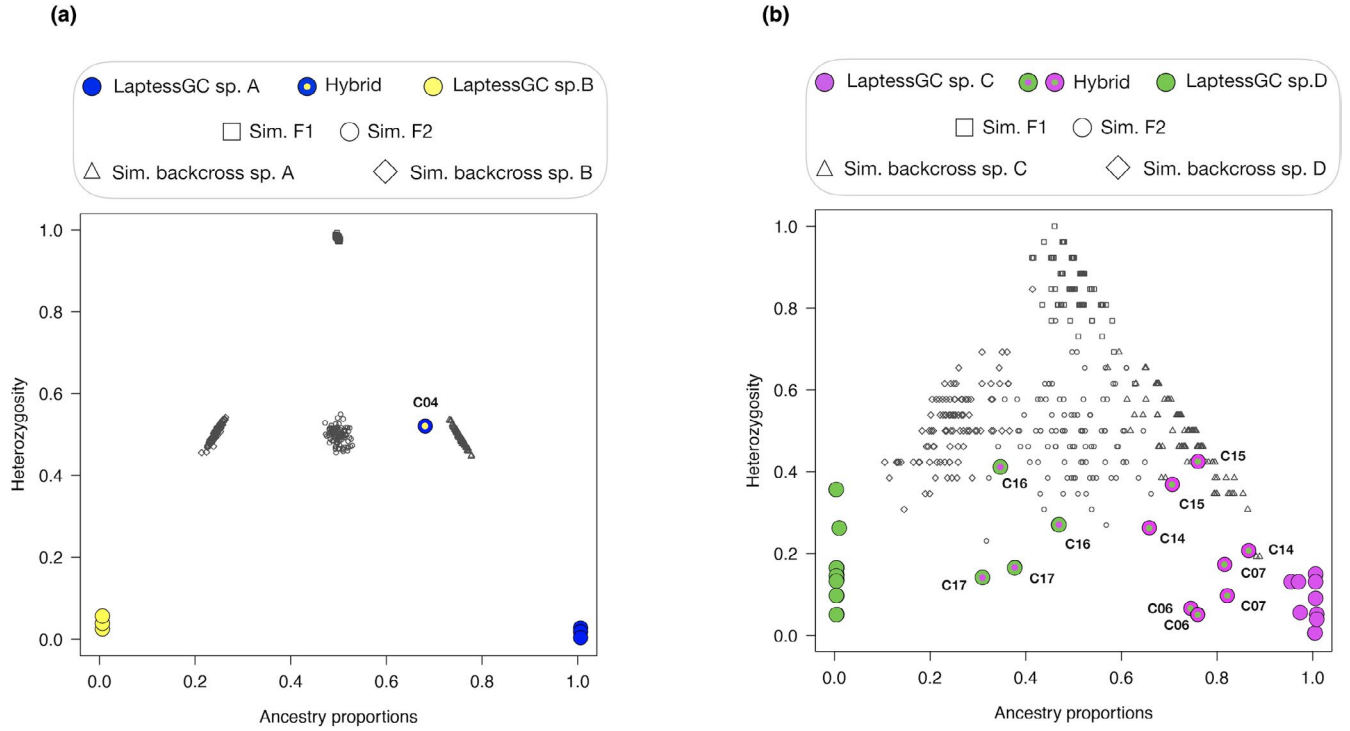

FIGURE 5 Hybrid genome simulations. Diagnostic loci from parental species are used to simulate expected genotypes for F1 and F2 hybrids, as well as F1 backcrosses with parental species. Sampling sites are indicated for admixed individuals (see Figure 2). (a) High diagnosability of different hybrid classes clearly identifies an individual derived from admixture between LaptessGC sp. A and LaptessGC sp. B as not being of recent hybrid origin. (b) Despite limited diagnosability, all individuals derived from admixture between LaptessGC sp. C and LaptessGC sp. D are inferred to be older than F1 hybrids, and a smaller number can be diagnosed as being older than second generation hybrids

settings and among islands, its potential role as a driver of speciation within islands has been overlooked. Here we have presented a conceptual model for species distribution responses to the changing geography of local climate, an insular topoclimate model for Quaternary diversification (ITQD), as glacial-scale climate change plays out over topographically complex island landscapes. Using the radially eroded conical landscape of Gran Canaria, our results provide support for the ITQD model, revealing a complex demographic history involving isolation, secondary contact and admixture. Signatures of admixture were associated with higher elevations, contrasting with an association of purer parental genomes at lower elevations, supporting prediction one. Higher genetic connectivity among individuals separated along an altitudinal axis compared to radial separation provides support for prediction two, while prediction three is unsupported, with no significant signatures for recent demographic expansion.

4.1 | Admixture

Our results reveal two clear cases of admixture, one of which is largely characterized by higher altitudes in the centre of the island, from 1,406 to 1,813 m above current sea level (m.a.c.s.l.), involving the parental species LaptessGC sp. C and LaptessGC sp. D that were sampled at lower altitudes, from 708 to 1,507 m.a.c.s.l. (Figure 4a). Specifically, LaptessGC sp. C is restricted to the northern and eastern slopes of Gran Canaria, while LaptessGC sp. D is restricted to southern slopes. To explain population purity at lower elevations with admixture at higher elevations requires that the distribution of either one or both species has moved upslope facilitating contact and admixture. This is consistent with expectations following the LGM, where warming temperatures would have acted to enforce upslope shifts in species ranges (Fernández-Palacios et al., 2016). Thus, the geography of admixture between LaptessGC sp. C and LaptessGC sp. D is consistent with a topoclimatic model.

Individuals derived from admixture between LaptessGC sp. C and LaptessGC sp. D were also sampled from two further sites, C06 and C07 (Figure 2). These two sites fall outside the combined sampled ranges of LaptessGC sp. C and LaptessGC sp. D, being associated with the north-western Tamadaba massif, where altitude rises again from approximately 1,000 m.a.c.s.l. to exceed 1,400 m.a.c.s.l. This regional topographic anomaly raises three possible explanations. The first is that there may be geographically close but unsampled pure parental populations in the Tamadaba region, consistent with recent (i.e. post LGM) admixture. The second possible explanation is that parental populations isolated locally during the LGM fully introgressed, which is again consistent with post LGM admixture. A third possible explanation is that admixture occurred prior to the LGM. Consistent with an older origin for the admixture of these populations is (a) their more distant relatedness to the parental populations in the PCA (Figure S2.4), and (b) their morphological differentiation from other individuals

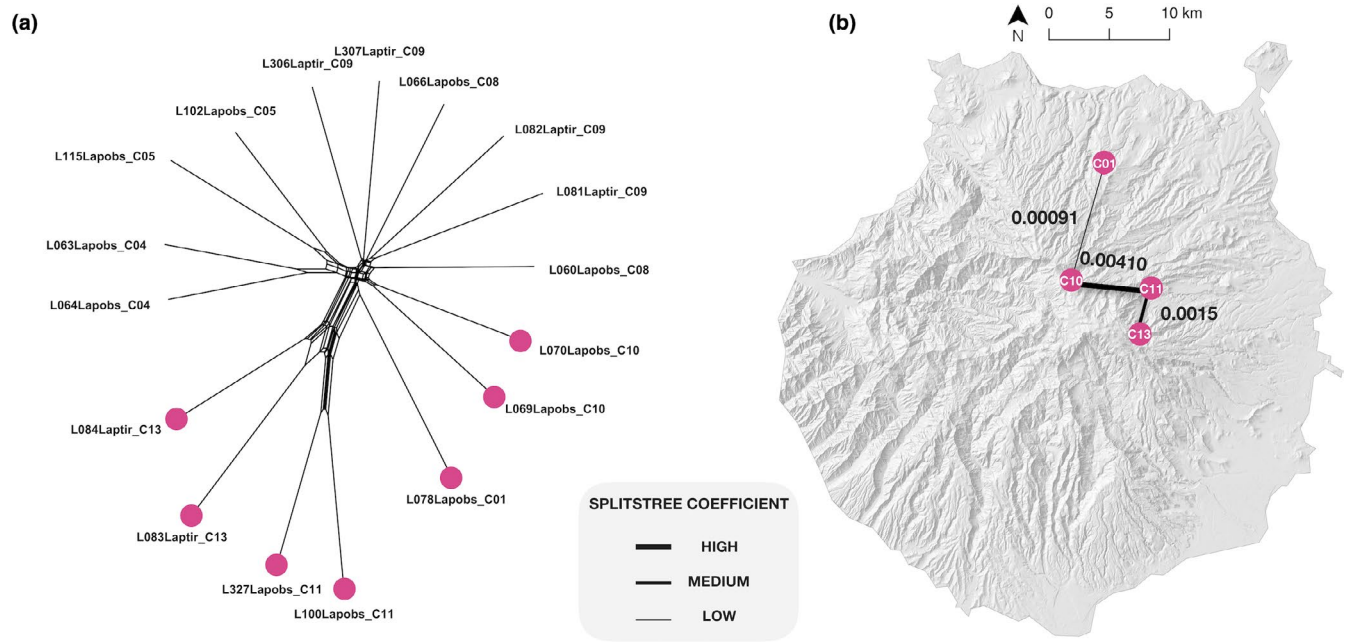

FIGURE 6 Altitudinal versus radial genomic relatedness. (a) Neighbour-Net phylogenetic network summarizing genomic relatedness among individuals from LaptessGC sp. C. Individuals highlighted in pink represent sampling sites that capture altitudinal and radial limits of the distribution and were used to estimate genomic distance. (b) Mean edge weights calculated from 100 bootstrapped data sets were used to estimate genomic distance per kilometre among sampling sites. Genomic distance between C01 and C10 (9.1E-4 ± 3.9.1E-4) is significantly lower ($p < 0.05$ based on a Nemenyi test for multiple comparisons) than between C10 and C11 (4.1E-3 ± 1.0E-3) and C11 and C13 (1.5E-3 ± 5.9E-4)

TABLE 2 Neutrality tests. Neutrality tests for the hypothesized species (see Table 1) in the *Laparocerus tessellatus* complex in Gran Canaria (genomic clusters identified in the PCA analyses are provided in brackets). All values for Tajima's *D* and Fu and Li's *D* are statistically non-significant ($p > .10$)

Genomic clusters	Tajima's *D*	Fu and Li's *D*
LaptessGC sp. A (G1)	−0.515	−0.291
LaptessGC sp. B (G3)	0.112	0.108
LaptessGC sp. C (G4)	−1.594	−1.846
LaptessGC sp. D (G6)	−0.728	−0.450

derived from admixture between LaptessGC sp. C and LaptessGC sp. D. Individuals from C06 and C07 are taxonomically described as *L. microphthalmus*, with the remaining admixed individuals from C14–C17 being taxonomically assigned to *L. tirajana*. To consider a dynamic under which genomic admixture might both arise during interglacial climatic conditions and persist through interglacial conditions, it is informative to draw comparison with population genetic expectations over glacial time-scales within continental settings.

4.2 | Admixture and persistence

There is a rich literature on species demographic responses to Quaternary climate change, particularly within palearctic settings (e.g. Hewitt, 2000, 2004), with much empirical data demonstrating a dynamic where populations restricted to southern refugial areas during glacial periods expand and extend their distributions north as interglacial conditions unfold. Similar to our insular topoclimatic model, such range expansions create the potential for secondary contact and hybridization, with many empirical examples of hybrid zones that have formed as a direct consequence of change in climate since the LGM (e.g. Hewitt, 2000, 2004). In a palearctic setting, such hybrid zones, and their genomic consequences, are transient. This transiency is a function of the typically vast distances between hybrid zones and refugial areas, separated by typically shallow elevational gradients. In the same way that post glacial northward range expansions from glacial refugia were typically rapid (Hewitt, 2000, 2004), so were southward contractions driven by the onset of glacial conditions, eliminating novel genomic variation from admixture as population extinction tracked south.

In an insular setting, the scale of range size change from glacial to interglacial conditions will be moderated by topography, whereby latitudinal and longitudinal changes are dampened by compensatory altitudinal shifts. It is this expectation for more limited change in the spatial dimensions of range size across glacial climate cycles, together with the potentially high topographic complexity within which these limited range changes may occur, that may facilitate the persistence of novel admixed genomic variation across glacial cycles. Under a conceptual model where favourable habitat downslope from admixed populations is occupied by parental populations, extinction of admixed genomic variation would seem

TABLE 3 Resistance analysis. Model rankings for landscape resistance variables tested against individual genomic relatedness for LaptessGC sp. A, LaptessGC sp. B, LaptessGC sp. C and LaptessGC sp. D, both with and without admixed individuals included. Only the five highest ranking models are presented in each case, with models identified as being optimal (ΔAIC_c ranges between 0–2) highlighted in bold. R^2m = marginal R^2 value; R^2c = conditional R^2 value; DIST = Euclidean distance, NULL = null model, P-LGM = mean annual precipitation at Last Glacial Maximum, (LGM) P-CT = contemporary mean annual precipitation, T-LGM = mean annual temperature at LGM, T-CT = mean annual temperature at current time, DEM = digital elevation model, TWI = topographic wetness index, TPI = topographic position index, TRI = topographic ruggedness index

Species	Variable	AIC_c	ΔAIC_c	R^2_m	R^2_c
LaptessGC sp. A	**DIST**	**−88.86**	**0.00**	**0.31**	**0.33**
	NULL	**−88.61**	**0.24**	**0.00**	**0.00**
	TRI	−51.02	37.83	0.41	0.41
	TWI	−50.04	38.82	0.36	0.36
	TPI	−49.60	39.25	0.34	0.34
LaptessGC sp. A without admixed individuals	**NULL**	**−97.85**	**0.00**	**0.00**	**0.92**
	DIST	**−97.52**	**0.33**	**0.01**	**0.94**
	TRI	−76.90	20.95	0.02	0.94
	TPI	−76.80	21.05	0.02	0.94
	P-CT	−76.78	21.06	0.02	0.94
LaptessGC sp. B	**DIST**	**−56.19**	**0.00**	**0.56**	**0.88**
	NULL	−42.60	13.60	0.00	0.15
	TPI	−30.71	25.48	0.84	0.96
	TWI	−25.14	31.05	0.80	0.95
	T-LGM	−19.90	36.29	0.58	0.93
LaptessGC sp. C	**P-LGM**	**−1,802.08**	**0.00**	**0.67**	**0.89**
	DEM	−1,699.34	102.74	0.56	0.90
	T-LGM	−1,690.64	111.44	0.54	0.91
	T-CT	−1,689.18	112.90	0.54	0.91
	TWI	−1,667.65	134.43	0.43	0.82
LaptessGC sp. C without admixed individuals	**P-LGM**	**−834.78**	**0.00**	**0.53**	**0.88**
	P-CT	−823.65	11.13	0.50	0.82
	DEM	−822.12	12.66	0.47	0.87
	TWI	−820.30	14.48	0.41	0.85
	P-LGM	−834.78	0.00	0.53	0.88
LaptessGC sp. D	**P-LGM**	**−339.60**	**0.00**	**0.68**	**0.89**
	TPI	−318.52	21.07	0.52	0.82
	DIST	−301.47	38.12	0.17	0.74
	TRI	−299.70	39.90	0.29	0.77
	TWI	−297.60	41.99	0.29	0.78
LaptessGC sp. D without admixed individuals	**NULL**	**−136.93**	**0.00**	**0.00**	**0.66**
	DIST	−133.74	3.18	0.02	0.67
	TWI	−118.00	18.93	0.55	0.65
	P-LGM	−114.32	22.60	0.05	0.69
	DEM	−114.13	22.79	0.07	0.63

probable, due to priority effects (Alford & Wilbur, 1985). However, under a model where favourable downslope habitat is unoccupied, and generation-scale climate change across latitudinal and longitudinal axes are less than dispersal distance, descendants of admixed origin may potentially track climate change and habitat suitability downslope (Figure 3). Under such a dynamic, the fate of admixed genomic variation from the four high altitude sampling sites of C14 to C17 (Figure 2), under a future climate cooling scenario with the next glacial event, need not necessarily be one of extinction.

Admixed genomes sampled between the ranges of LaptessGC sp. C and LaptessGC sp. D span a geographic distance of *c*. 7 km. Although we cannot definitively exclude that all favourable habitat downslope of the admixed range is populated by parental genotypes, it is improbable given the results of historical sampling efforts (AMC, unpublished data). Thus, there is potential for downslope movement of admixed genomes, and their survival through glacial maxima, providing a plausible mechanistic explanation for geographically disjunct populations of admixed genomes, such as those from the westernmost sampling sites (C06 and C07).

4.3 | Admixture, persistence and speciation

It has recently been noted that admixture between divergent genomes could be a consequential process for insular speciation,

potentially catalysing adaptive change and speciation (Emerson & Faria, 2014), and the more prevalent dynamic underpinning genomic admixture has been secondary contact arising from sequential colonization of the same island by the same source species (e.g. Faria et al., 2016; Garrick et al., 2014; Jordal et al., 2006; Nietlisbach et al., 2013; Shaw, 2002). To our knowledge, our results are the first compelling evidence of genomic admixture within an island, without colonization. Aside from the adaptive implications of admixture (Emerson & Faria, 2014), neutral processes of drift and recombination within admixed gene pools may also facilitate speciation through the generation of haplotypes and gene combinations that are incompatible with those of parental populations (Abbott et al., 2013). Thus, the persistence of admixed gene pools through time may contribute to both neutral and adaptive speciation.

The long-term fate of the admixed gene pools between LaptessGC sp. C and LaptessGC sp. D can only be speculated upon. Although there is tentative support for the admixed gene pools of the geographically disjunct populations of C06 and C07 having persisted through the LGM, the longer term consequences of this, in terms of island community assembly, are unclear. Fortuitously the second admixture event that our analyses uncovered, involving the parental species LaptessGC sp. A and LaptessGC sp. B, provides some additional insight into community assembly consequences of admixture. The two parental species present similar distribution ranges in the northern slopes of the island, with our sampling suggesting them to be allopatric at the local scale (Figure 4c). A strong signature of admixture between both parental genomes was revealed within an individual sampled at site C04. The sympatry of the admixed individual together with one of the parental species, LaptessGC sp. A, and a non-parental species, LaptessGC sp. C, suggests that this admixed individual may belong to a fifth putative biological species, highlighting the potential for long-term persistence of admixed genomes, and their role in the origin of new species. However, further sampling of admixed individuals derived from LaptessGC sp. A and LaptessGC sp. B is required for a more robust inference.

4.4 | Changing Quaternary bioclimate landscapes as drivers of population isolation and contact

The ITQD model makes the general prediction that connectivity between valleys within a conically shaped island is enhanced during interglacial conditions, as favourable climate is pushed upslope, where topographic heterogeneity, and thus environmental distance, is reduced among populations. In contrast, connectivity within valleys would remain relatively unchanged between both glacial and interglacial conditions, with the model making the general prediction that range limits should shift upslope. The species LaptessGC sp. C, which shows the broadest geographic distribution, revealed higher genetic connectivity among sites distributed along an altitudinal transect compared to populations separated radially around the island. These results are consistent with the prediction from the ITQD model that changes in climate throughout the Quaternary would result in higher potential bioclimate connectivity within valleys than among valleys. Indeed, topographic positions, such as valley bottoms and basins, have been highlighted as ideal environments for microrefugia during Pleistocene glacial cycles (Dobrowski, 2011).

Landscape resistance analyses to test among mechanistic models for spatial structuring of genomic variation revealed evidence for geographic variation of annual precipitation during the LGM explaining contemporary geographic patterns of individual genomic relatedness. Admixed individuals assigned to either LaptessGC sp. C or LaptessGC sp. D were sampled from higher elevation areas characterized by high precipitation during the LGM. This is consistent with the origin of admixed individuals by upslope movement, and eventual secondary contact of parental species in response to less humid conditions upslope as glacial conditions transitioned to interglacial. Phenological data for *Laparocerus* suggests that reduced levels of precipitation at higher altitudes are likely to have contributed to this dynamic together with increased temperature. Adult activity of *Laparocerus* species is typically concentrated in the more humid winter months. The few species whose maximum numbers shift to spring or early summer are notably found at higher elevations, where low winter temperatures are suggested to be a limiting factor (Machado & Aguiar, 2005).

None of the four species analysed presented significant support for recent demographic expansion from a bottleneck, although seven of eight analyses presented values suggestive of expansion. These results perhaps highlight the complexity of demographic prediction within an insular geographic context. In the absence of a detailed understanding of probable species ranges during glacial climate conditions, it may be that simple predictions of demographic expansion are unrealistic. Upslope shifts in distribution limits may entail only limited increases in overall population size, compared to latitudinal range expansions in continental settings. An additional complication is that higher altitudes are precisely those areas where signatures for demographic expansion are expected to be strongest. However, estimation of any such signal would be further complicated by the existence of admixture at higher altitudes, and the necessary removal of such admixed individuals from demographic analyses, as was the case for two of our four species.

5 | CONCLUSIONS

Our topoclimatic model for insular diversification places emphasis on the role of topography and changes in climate throughout the Quaternary for the process of diversification within islands. Using RAD-seq data for a beetle taxon with low-dispersal ability and affinity for areas of higher humidity within the pluviseasonal bioclimate of Gran Canaria, we found general support for the ITQD model, with evidence for isolation and admixture consistent with expectations as climate transitions between glacial and interglacial conditions. With regard to the generality of our model, it is likely to be less consequential within islands that present little topographic complexity, or for species that are highly dispersive, or with broad environmental

tolerances. However, as topographic complexity increases, and as species traits tend towards low dispersal ability and limited environmental tolerances, we suggest the ITQD model will be a useful framework for interpreting patterns of genomic relatedness across insular landscapes.

ACKNOWLEDGEMENTS

The authors acknowledge the contribution of the Teide High-Performance Computing facility (TeideHPC) provided by the Instituto Tecnológico y de Energías Renovables (ITER), S.A., and the City University of New York High Performance Computing Center, with support from the National Science Foundation (CNS-0855217 and CNS-0958379). This work was supported by the Spanish Ministerio de Economía y Competitividad (MINECO) grants CGL2013-42589-P and CGL2017-85718-P, co-financed by FEDER. V.G.O. is funded by a MINECO FPI contract and J.P. was funded by the MINECO through the Juan de la Cierva Program—Incorporation (IJCI-2014-19691) and Ramón y Cajal Program (RYC-2016-20506), and Marie Sklodowska-Curie COFUND, Researchers' Night and Individual Fellowships Global (MSCA grant agreement no. 747238, "UNISLAND"). Fieldwork was supported by collecting permit 167/15 kindly provided by the Cabildo of Gran Canaria. We wish to thank Heriberto López for help with sampling, sample identification, and assistance with laboratory work. Finally, we also thank two anonymous reviewers for comments on a previous version of the manuscript.

DATA AVAILABILITY STATEMENT

Raw Illumina reads deposited in the NCBI Sequence Read Archive (PRJNA556326). We provide a package on DRYAD (https://doi.org/10.5061/dryad.bs2gh38) that includes our final RAD-seq filtered genotypes and input files for the following analyses: sNMF, PCA, SNAPP, HYBRIDLAB SPLITSTREE, ARLEQUIN.

ORCID

Jairo Patiño https://orcid.org/0000-0001-5532-166X
Isaac Overcast https://orcid.org/0000-0001-8614-6892
Brent C. Emerson https://orcid.org/0000-0003-4067-9858

REFERENCES

Abbott, R., Albach, D., Ansell, S., Arntzen, J. W., Baird, S. J. E., Bierne, N., … Zinner, D. (2013). Hybridization and speciation. *Journal of Evolutionary Biology*, *26*, 229–246. https://doi.org/10.1111/j.1420-9101.2012.02599.x

Alford, R. A., & Wilbur, H. M. (1985). Priority effects in experimental pond communities: Competition between *Bufo* and *Rana*. *Ecology*, *66*, 1097–1105. https://doi.org/10.2307/1939161

Ali, J. R., & Aitchison, J. C. (2014). Exploring the combined role of eustasy and oceanic island thermal subsidence in shaping biodiversity on the Galápagos. *Journal of Biogeography*, *41*, 1227–1241. https://doi.org/10.1111/jbi.12313

Anguita, F., Márquez, A., Castiñeiras, P., & Hernán, F. (2002). *Los Volcanes de Canarias. Guía geológica e itinerarios*. Madrid, Spain: Ed. Rueda.

Aulinas, M., Gimeno, D., Fernandez-Turiel, J. L., Perez-Torrado, F. J., Rodriguez-Gonzalez, A., & Gasperini, D. (2010). The Plio-Quaternary magmatic feeding system beneath Gran Canaria (Canary Islands, Spain): Constraints from thermobarometric studies. *Journal of the Geological Society*, *167*, 785–801. https://doi.org/10.1144/0016-76492009-184

Bates, D. M., Maechler, M., Bolker, B. M., & Walker, S. (2014). lme4: Linear mixed-effects models using Eigen and S4 (Version R package version 1.1-6). Retrieved from http://CRAN.R-project.org/package=lme4

Brown, R. M., & Diesmos, A. C. (2002). Application of lineage-based species concepts to oceanic island frog populations: The effects of differing taxonomic philosophies on the estimation of Philippine biodiversity. *Silliman Journal*, *42*, 133–162.

Brown, R. M., Siler, C. D., Diesmos, A. C., & Alcala, A. C. (2009). Philippine frogs of the genus *Leptobrachium* (Anura; Megophryidae): Phylogeny-based species delimitation, taxonomic review, and descriptions of three new species. *Herpetological Monographs*, *23*, 1–44. https://doi.org/10.1655/09-037.1

Bryant, D., Bouckaert, R., Felsenstein, J., Rosenberg, N. A., & RoyChoudhury, A. (2012). Inferring species trees directly from biallelic genetic markers: Bypassing gene trees in a full coalescent analysis. *Molecular Biology and Evolution*, *29*, 1917–1932. https://doi.org/10.1093/molbev/mss086

Carracedo, J. C., & Day, S. (2002). *Canary Islands. Classic geology in Europe series*, Vol. 4. Harpenden: Terra Publishing.

Carracedo, J., & Troll, V. (2016). *The geology of the Canary Islands*. Amsterdam: Elsevier.

Casquet, J., Thebaud, C., & Gillespie, R. G. (2012). Chelex without boiling, a rapid and easy technique to obtain stable amplifiable DNA from small amounts of ethanol-stored spiders. *Molecular Ecology Resources*, *12*, 136–141. https://doi.org/10.1111/j.1755-0998.2011.03073.x

Contreras-Diaz, H. G., Moya, O., Oromi, P., & Juan, C. (2007). Evolution and diversification of the forest and hypogean ground-beetle genus *Trechus* in the Canary Islands. *Molecular Phylogenetics and Evolution*, *42*, 687–699. https://doi.org/10.1016/j.ympev.2006.10.007

Danecek, P., Auton, A., Abecasis, G., Albers, C. A., Banks, E., DePristo, M. A., … Durbin, R. (2011). The variant call format and VCFTOOLS. *Bioinformatics*, *27*, 2156–2158. https://doi.org/10.1093/bioinformatics/btr330

Danielson, J. J. & Gesch, D. B. (2011) Global multi-resolution terrain elevation data 2010 (GMTED2010). In U.S. Geological Survey (Series Ed.) & E. R. O. a. S. E. Center (Vol. Ed.). U.S. Geological Survey Open-File Report (pp. 26).

del-Arco, M., Salas, M., Acebes, J. R., del C. Marrero, M., Reyes-Betancort, J. A., & Pérez-de-Paz, J. A. (2002). Bioclimatology and climatophilous vegetation of Gran Canaria (Canary Islands). *Annales Botanici Fennici*, *39*, 15–41.

Dimitrov, D., Arnedo, M. A., & Ribera, C. (2008). Colonization and diversification of the spider genus *Pholcus* Walckenaer, 1805 (Araneae, Pholcidae) in the Macaronesian archipelagos: Evidence for long-term occupancy yet rapid recent speciation. *Molecular Phylogenetics and Evolution*, *48*, 596–614. https://doi.org/10.1016/j.ympev.2008.04.027

Dobrowski, S. Z. (2011). A climatic basis for microrefugia: The influence of terrain on climate. *Global Change Biology*, *17*, 1022–1035. https://doi.org/10.1111/j.1365-2486.2010.02263.x

Eaton, D. A. R., & Overcast, I. (2016). ipyrad: Interactive assembly and analysis of RADseq data sets. Retrieved fromhttp://ipyrad.readthedocs.io/

Emerson, B. C. (2003). Genes, geology and biodiversity: Faunal and floral diversity on the island of Gran Canaria. *Animal Biodiversity and Conservation*, *26*, 9–20.

Emerson, B. C., & Faria, C. M. (2014). Fission and fusion in island taxa–serendipity, or something to be expected? *Molecular Ecology*, *23*, 5132–5134. https://doi.org/10.1111/mec.12951

Emerson, B. C., & Gillespie, R. G. (2008). Phylogenetic analysis of community assembly and structure over space and time. *Trends in Ecology & Evolution*, *23*, 619–630. https://doi.org/10.1016/j.tree.2008.07.005

Emerson, B. C., & Oromi, P. (2005). Diversification of the forest beetle genus *Tarphius* on the Canary Island, and the evolutionary origins of island endemics. *Evolution*, *59*, 586–598.

Esselstyn, J. A., & Brown, R. M. (2009). The role of repeated sea-level fluctuations in the generation of shrew (Soricidae: *Crocidura*) diversity in the Philippine Archipelago. *Molecular Phylogenetics and Evolution*, *53*, 171–181. https://doi.org/10.1016/j.ympev.2009.05.034

Faria, C. M. A., Machado, A., Amorim, I. R., Gage, M. J. G., Borges, P. A. V., & Emerson, B. C. (2016). Evidence for multiple founding lineages and genetic admixture in the evolution of species within an oceanic island weevil (Coleoptera, Curculionidae) super-radiation. *Journal of Biogeography*, *43*, 178–191. https://doi.org/10.1111/jbi.12606

Fernández-Palacios, J. M., Rijsdijk, K. F., Norder, S. J., Otto, R., de Nascimento, L., Fernández-Lugo, S., … Whittaker, R. J. (2016). Towards a glacial-sensitive model of island biogeography. *Global Ecology and Biogeography*, *25*, 817–830.

Frichot, E., François, O., & O'Meara, B. (2015). LEA: An R package for landscape and ecological association studies. *Methods in Ecology and Evolution*, *6*, 925–929.

Frichot, E., Mathieu, F., Trouillon, T., Bouchard, G., & Francois, O. (2014). Fast and efficient estimation of individual ancestry coefficients. *Genetics*, *196*, 973–983. https://doi.org/10.1534/genetics.113.160572

Fu, Y. X., & Li, W. H. (1993). Statistical tests of neutrality of mutations. *Genetics*, *133*, 693–709.

García-Olivares, V., López, H., Patiño, J., Alvarez, N., Machado, A., Carracedo, J. C., … Emerson, B. C. (2017). Evidence for mega-landslides as drivers of island colonization. *Journal of Biogeography*, *44*, 1053–1064. https://doi.org/10.1111/jbi.12961

Garrick, R. C., Benavides, E., Russello, M. A., Hyseni, C., Edwards, D. L., Gibbs, J. P., … Caccone, A. (2014). Lineage fusion in Galápagos giant tortoises. *Molecular Ecology*, *23*, 5276–5290. https://doi.org/10.1111/mec.12919

Gillespie, R. G., & Roderick, G. K. (2014). Geology and climate drive diversification. *Nature*, *509*, 297. https://doi.org/10.1038/509297a

Goodman, K. R., Welter, S. C., & Roderick, G. K. (2012). Genetic divergence is decoupled from ecological diversification in the Hawaiian *Nesosydne* planthoppers. *Evolution*, *66*, 2798–2814. https://doi.org/10.1111/j.1558-5646.2012.01643.x

Guillou, H., Torrado, F. J. P., Hansen Machin, A. R., Carracedo, J. C., & Gimeno, D. (2004). The Plio-Quaternary volcanic evolution of Gran Canaria based on new K-Ar ages and magnetostratigraphy. *Journal of Volcanology and Geothermal Research*, *135*, 221–246. https://doi.org/10.1016/j.jvolgeores.2004.03.003

Heaney, L. R. (1985). Zoogeographic evidence for middle and late Pleistocene land bridges to the Philippine Islands. *Modern Quaternary Research in Southeast Asia*, *9*, 127–144.

Hendrickx, F., Backeljau, T., Dekoninck, W., Van Belleghem, S. M., Vandomme, V., & Vangestel, C. (2015). Persistent inter- and intraspecific gene exchange within a parallel radiation of caterpillar hunter beetles (*Calosoma* sp.) from the Galapagos. *Molecular Ecology*, *24*, 3107–3121.

Hewitt, G. M. (2000). The genetic legacy of the Quaternary ice ages. *Nature*, *405*, 907–913. https://doi.org/10.1038/35016000

Hewitt, G. M. (2004). Genetic consequences of climatic oscillations in the Quaternary. *Philosophical Transactions of the Royal Society B: Biological Sciences*, *359*, 183–195. https://doi.org/10.1098/rstb.2003.1388

Huson, D. H., & Bryant, D. (2006). Application of phylogenetic networks in evolutionary studies. *Molecular Biology and Evolution*, *23*, 254–267. https://doi.org/10.1093/molbev/msj030

Jombart, T., & Ahmed, I. (2011). adegenet 1.3-1: New tools for the analysis of genome-wide SNP data. *Bioinformatics*, *27*, 3070–3071. https://doi.org/10.1093/bioinformatics/btr521

Jombart, T., & Collins, C. (2015). A tutorial for discriminant analysis of principal components (DAPC) using adegenet 2.0.0. Retrieved from: http://adegenet.r-forge.r-project.org/files/tutorial-dapc.pdf43.

Jordal, B. H., Emerson, B. C., & Hewitt, G. M. (2006). Apparent 'sympatric' speciation in ecologically similar herbivorous beetles facilitated by multiple colonizations of an island. *Molecular Ecology*, *15*, 2935–2947. https://doi.org/10.1111/j.1365-294X.2006.02993.x

Jordan, S., Simon, C., Foote, D., & Englund, R. A. (2005). Phylogeographic patterns of Hawaiian Megalagrion damselflies (Odonata: Coenagrionidae) correlate with Pleistocene island boundaries. *Molecular Ecology*, *14*, 3457–3470. https://doi.org/10.1111/j.1365-294X.2005.02669.x

Karátson, D., Yepes, J., Favalli, M., Rodríguez-Peces, M. J., & Fornaciai, A. (2016). Reconstructing eroded paleovolcanoes on Gran Canaria, Canary Islands, using advanced geomorphometry. *Geomorphology*, *253*, 123–134. https://doi.org/10.1016/j.geomorph.2015.10.004

Karger, D. N., Conrad, O., Böhner, J., Kawohl, T., Kreft, H., Soria-Auza, R. W., … Kessler, M. (2017). Climatologies at high resolution for the earth's land surface areas. *Scientific Data*, *4*, 170122. https://doi.org/10.1038/sdata.2017.122

Katoh, K., Misawa, K., Kuma, K. I., & Miyata, T. (2002). MAFFT: A novel method for rapid multiple sequence alignment based on fast Fourier transform. *Nucleic Acids Research*, *30*, 3059–3066. https://doi.org/10.1093/nar/gkf436

Kearse, M., Moir, R., Wilson, A., Stones-Havas, S., Cheung, M., Sturrock, S., … Drummond, A. (2012). Geneious Basic: An integrated and extendable desktop software platform for the organization and analysis of sequence data. *Bioinformatics*, *28*, 1647–1649. https://doi.org/10.1093/bioinformatics/bts199

Leache, A. D., Fujita, M. K., Minin, V. N., & Bouckaert, R. R. (2014). Species delimitation using genome-wide SNP data. *Systematic Biology*, *63*, 534–542. https://doi.org/10.1093/sysbio/syu018

Machado, A., & Aguiar, A. (2005). Phenology of *Laparocerus* species in Tenerife, Canary Islands (Coleoptera, Curculionidae). *Boletim do Museu Municipal do Funchal*, *56*, 5–21.

Machado, A., Rodriguez-Exposito, E., Lopez, M., & Hernandez, M. (2017). Phylogenetic analysis of the genus *Laparocerus*, with comments on colonisation and diversification in Macaronesia (Coleoptera, Curculionidae, Entiminae). *ZooKeys*, *651*, 1–77. https://doi.org/10.3897/zookeys.651.10097

Mastretta-Yanes, A., Arrigo, N., Alvarez, N., Jorgensen, T. H., Pinero, D., & Emerson, B. C. (2015). Restriction site-associated DNA sequencing, genotyping error estimation and de novo assembly optimization for population genetic inference. *Molecular Ecology Resources*, *15*, 28–41.

McRae, B. H. (2006). Isolation by resistance. *Evolution*, *60*, 1551–1561. https://doi.org/10.1111/j.0014-3820.2006.tb00500.x

McRae, B. H., Dickson, B. G., Keitt, T. H., & Shah, V. B. (2008). Using circuit theory to model connectivity in ecology, evolution, and conservation. *Ecology*, *89*, 2712–2724. https://doi.org/10.1890/07-1861.1

Nazareno, A. G., Bemmels, J. B., Dick, C. W., & Lohmann, L. G. (2017). Minimum sample sizes for population genomics: An empirical study from an Amazonian plant species. *Molecular Ecology Resources*, *17*, 1136–1147. https://doi.org/10.1111/1755-0998.12654

Nielsen, E. E., Bach, L. A., & Kotlicki, P. (2006). Hybridlab (version 1.0): A program for generating simulated hybrids from population samples. *Molecular Ecology Notes*, *6*, 971–973. https://doi.org/10.1111/j.1471-8286.2006.01433.x

Nietlisbach, P., Wandeler, P., Parker, P. G., Grant, P. R., Grant, B. R., Keller, L. F., & Hoeck, P. E. (2013). Hybrid ancestry of an island subspecies of Galapagos mockingbird explains discordant gene trees. *Molecular Phylogenetics and Evolution*, *69*, 581–592.

Norder, S. J., Proios, K., Whittaker, R. J., Alonso, M. R., Borges, P. A. V., Borregaard, M. K., … Rijsdijk, K. F. (2019). Beyond the Last Glacial Maximum: Island endemis is best exlained by long-lasting archipelago configurations. *Global Ecology and Biogeography*, *28*, 184–197.

Papadopoulou, A., & Knowles, L. L. (2015a). Genomic tests of the species-pump hypothesis: Recent island connectivity cycles drive population divergence but not speciation in Caribbean crickets across the Virgin Islands. *Evolution*, *69*, 1501–1517. https://doi.org/10.1111/evo.12667

Papadopoulou, A., & Knowles, L. L. (2015b). Species-specific responses to island connectivity cycles: Refined models for testing phylogeographic concordance across a Mediterranean Pleistocene Aggregate Island Complex. *Molecular Ecology*, *24*, 4252–4268. https://doi.org/10.1111/mec.13305

Patiño, J., Whittaker, R. J., Borges, P. A. V., Fernández-Palacios, J. M., Ah-Peng, C., Araújo, M. B., … Emerson, B. C. (2017). A roadmap for island biology: 50 fundamental questions after 50 years of The Theory of Island Biogeography. *Journal of Biogeography*, *44*, 963–983.

Pérez-Torrado, F. J., Carracedo, J. C., & Mangas, J. (1995). Geochronology and stratigraphy of the Roque Nublo Cycle, Gran Canaria, Canary Islands. *Journal of the Geological Society*, *152*, 807–818. https://doi.org/10.1144/gsjgs.152.5.0807

Peterman, W. E. (2018). ResistanceGA: An R package for the optimisation of resistance surfaces using genetic algorithms. *Methods in Ecology and Evolution*, *9*, 1638–1647.

Peterman, W. E., Connette, G. M., Keitt, T. H., & Shah, V. B. (2014). Ecological resistance surfaces predict fine-scale genetic differentiation in a terrestrial woodland salamander. *Molecular Ecology*, *23*, 2402–2413. https://doi.org/10.1111/mec.12747

Peterson, B. K., Weber, J. N., Kay, E. H., Fisher, H. S., & Hoekstra, H. E. (2012). Double digest RADseq: An inexpensive method for de novo SNP discovery and genotyping in model and non-model species. *PLoS ONE*, *7*, e37135. https://doi.org/10.1371/journal.pone.0037135

Petkova, D., Novembre, J., & Stephens, M. (2015). Visualising spatial population structure with estimated effective migration surfaces. *Nature Genetics*, *48*, 94–100.

R Core Team (2013). *R: A language and environment for statistical computing*. Vienna, Austria: R Foundation for Statistical Computing. http://www.R-project.org/

Rambaut, A., & Drummond, A. (2014). FigTree vol 1.4.2: Tree Figure Drawing Tool. Retrieved from http://tree.bio.ed.ac.uk/software/figtree

Rambaut, A., Drummond, A. J., Xie, D., Baele, G., & Suchard, M. A. (2018). Posterior summarisation in Bayesian phylogenetics using Tracer 1.7. *Systematic Biology*, *65*, 901–904.

Rijsdijk, K. F., Hengl, T., Norder, S. J., Otto, R., Emerson, B. C., Ávila, S. P., … Fernández-Palacios, J. M. (2014). Quantifying surface-area changes of volcanic islands driven by Pleistocene sea-level cycles: Biogeographical implications for the Macaronesian archipelagos. *Journal of Biogeography*, *41*, 1242–1254. https://doi.org/10.1111/jbi.12336

Rodriguez-Gonzalez, A., Fernandez-Turiel, J. L., Perez-Torrado, F. J., Paris, R., Gimeno, D., Carracedo, J. C., & Aulinas, M. (2012). Factors controlling the morphology of monogenetic basaltic volcanoes: The Holocene volcanism of Gran Canaria (Canary Islands, Spain). *Geomorphology*, *136*, 31–44. https://doi.org/10.1016/j.geomorph.2011.08.023

Ronquist, F., Teslenko, M., van der Mark, P., Ayres, D. L., Darling, A., Höhna, S., … Huelsenbeck, J. P. (2012). MrBayes 3.2: Efficient Bayesian phylogenetic inference and model choice across a large model space. *Systematic Biology*, *61*, 539–542. https://doi.org/10.1093/sysbio/sys029

Rozas, J., Ferrer-Mata, A., Sanchez-DelBarrio, J. C., Guirao-Rico, S., Librado, P., Ramos-Onsins, S. E., & Sanchez-Gracia, A. (2017). DnaSP 6: DNA sequence polymorphism analysis of large data sets. *Molecular Biology and Evolution*, *34*, 3299–3302. https://doi.org/10.1093/molbev/msx248

Sequeira, A. S., Lanteri, A. A., Albelo, L. R., Bhattacharya, S., & Sijapati, M. (2008). Colonization history, ecological shifts and diversification in the evolution of endemic Galápagos weevils. *Molecular Ecology*, *17*, 1089–1107. https://doi.org/10.1111/j.1365-294X.2007.03642.x

Shapiro, L. H., Strazanac, J. S., & Roderick, G. K. (2006). Molecular phylogeny of *Banza* (Orthoptera: Tettigoniidae), the endemic katydids of the Hawaiian Archipelago. *Molecular Phylogenetics and Evolution*, *41*, 53–63. https://doi.org/10.1016/j.ympev.2006.04.006

Shaw, K. L. (2002). Conflict between nuclear and mitochondrial DNA phylogenies of a recent species radiation: What mtDNA reveals and conceals about modes of speciation in Hawaiian crickets. *Proceedings of the National Academy of Sciences*, *99*, 16122–16127. https://doi.org/10.1073/pnas.242585899

Shaw, K. L., & Gillespie, R. G. (2016). Comparative phylogeography of oceanic archipelagos: Hotspots for inferences of evolutionary process. *Proceedings of the National Academy of Sciences*, *113*, 7986–7993. https://doi.org/10.1073/pnas.1601078113

Tajima, F. (1989). Statistical method for testing the neutral mutation hypothesis by DNA polymorphism. *Genetics*, *123*, 585–595.

Vandergast, A. G., Gillespie, R. G., & Roderick, G. K. (2004). Influence of volcanic activity on the population genetic structure of Hawaiian *Tetragnatha* spiders: Fragmentation, rapid population growth and the potential for accelerated evolution. *Molecular Ecology*, *13*, 1729–1743. https://doi.org/10.1111/j.1365-294X.2004.02179.x

Weigelt, P., Steinbauer, M. J., Cabral, J. S., & Kreft, H. (2016). Late Quaternary climate change shapes island biodiversity. *Nature*, *532*, 99–102. https://doi.org/10.1038/nature17443

BIOSKETCH

The research team have complementary interests in the geology and biodiversity of oceanic islands, and the application of molecular data to understand the origin and maintenance of species and communities of species. This work is a synthesis of these different interests.

Author contributions: B.C.E., V.G.O. and J.P. designed the research project. B.C.E. & M.J.H. conducted fieldwork, with guidance from A.M. Laboratory work was conducted by V.G.O with assistance from J.P. Data processing and analyses were conducted by V.G.O., with input and assistance from B.C.E., J.P., I.O., M.H., A.S.C., U.L.H. and F.M.M. B.C.E and V.G.O wrote the manuscript, with input from J.P., and contributions from all authors.

SUPPORTING INFORMATION

Additional supporting information may be found online in the Supporting Information section at the end of the article.

How to cite this article: García-Olivares V, Patiño J, Overcast I, et al. A topoclimate model for Quaternary insular speciation. *J Biogeogr*. 2019;46:2769–2786. https://doi.org/10.1111/jbi.13689